BOSQUE
The Forest Journal of the Southern Hemisphere

DOI: 10.4206/Bosque.e4709
Climate modeling of Brazilian ipês

Original Articles

A modeling framework to assess climate vulnerability and future distributions of tropical tree species: a case study on Brazilian ipês

Fábio de Castro Borba [a], Caroline de Souza Bezerra [a], Jennifer Souza Tomaz [a], Maria José Marques [a], Helinara Lais Vieira Capucho [a], Samuel Freitas de Souza [a], Santiago Linorio Ferreyra Ramos [b], Ricardo Lopes [c], Carlos Henrique Salvino Gadelha de Meneses [d], Maria Teresa Gomes Lopes [a]*

[a] Federal University of Amazonas, Faculty of Agricultural Sciences, Department of Animal and Vegetable Production, Laboratory of Plant Genetics and Breeding, Manaus, Brazil.
[b] Brazilian Agricultural Research Corporation, Embrapa Western Amazon, Manaus, Brazil.
[c] Brazilian Agricultural Research Company, Agroforestry Research Center of the Western Amazon, Manaus, Brazil.
[d] Center for Biological and Health Sciences, Department of Biology, State University of Paraíba, Campina Grande, Brazil.

Article Info

Received: 09.03.2026
Accepted: 08.06.2026
Published: 22-06-2026

Corresponding author: mtglopes@ufam.edu.br

How to cite: de Castro Borba F., de Souza Bezerra C., Souza Tomaz J., Marques M. J., Vieira Capucho H. L., Freitas de Souza S., Ferreyra Ramos S. L., Lopes R., Salvino Gadelha de Meneses C. H., Gomes Lopes M. T. (2026). A modeling framework to assess climate vulnerability and future distributions of tropical tree species: a case study on Brazilian ipês. BOSQUE, 47, e4709.

https://doi.org/10.4206/Bosque.e4709

Abstract

Assessing climate vulnerability of tropical trees requires ecological niche modeling frameworks capable of integrating multiple sources of uncertainty. Here, we present an integrated modeling approach that combines climatic, edaphic, and topographic predictors, dimensionality reduction, multi-algorithm calibration, and ensemble forecasting to evaluate future environmental suitability under climate change. Using two Brazilian *Handroanthus* species as a case study, occurrence data were spatially filtered, predictors were summarized through principal component analysis, and models were built using six algorithms with performance-weighted consensus projections. Future distributions were projected for three time periods (2041–2060, 2061–2080, and 2081–2100) under intermediate and high emission scenarios (SSP2-4.5 and SSP5-8.5). The framework showed high predictive reliability and revealed contrasting vulnerability patterns, including severe suitability losses for one species and greater stability for the other across phytogeographic domains. Beyond species-specific outcomes, results demonstrate how integrated Ecologial Niche Modeling (ENM) frameworks can identify climate-driven risk gradients and support climate-informed conservation, forest management, and territorial planning in tropical regions.

Keywords: Handroanthus spp., climate change, forest resources.

DOI: 10.4206/Bosque.e4709

Introduction

Ecological niche modeling (ENM) is a widely used tool for understanding species distribution patterns, identifying environmentally suitable areas, and projecting potential shifts under future climate change scenarios (Fadda et al., 2026; Xu et al., 2025). By integrating climatic, edaphic, and topographic variables, ENM supports the assessment of species–environment relationships across broad spatial scales and provides relevant information for conservation planning (Thuiller, 2024). However, modeling tropical tree species remains challenging due to high dimensionality and collinearity among predictors, algorithm-related uncertainty, and the need for robust validation frameworks capable of producing reliable future projections.

Recent studies demonstrate that ENM performance and ecological realism are strongly influenced by methodological decisions, particularly variable selection, dimensionality reduction, and the choice of algorithms (Andrade et al., 2020; Thuiller, 2024). In tropical ecosystems, soil and geomorphological factors interact with climate to shape species distributions, yet they are often underrepresented in large-scale models. The inclusion of edaphic variables alongside climatic predictors improves model accuracy and ecological interpretability, especially for tree species whose establishment depends on soil texture, fertility, and water availability (Alvarez et al., 2022; Velazco et al., 2017). Approaches that summarize correlated environmental predictors into orthogonal components, such as Principal Component Analysis (PCA), combined with consensus modeling using multiple algorithms, have been recommended to reduce dimensionality, represent major environmental gradients, and increase projection robustness (Magalhães et al., 2025; Marmion et al., 2009).

Tropical tree species are particularly sensitive to climate change due to long life cycles, slow growth rates, and limited capacity to adjust rapidly to altered temperature and precipitation regimes. Climatic changes can disrupt physiological and phenological processes, reduce recruitment, and intensify exposure to abiotic stresses such as water deficit and soil degradation (Bauman et al., 2022; Malecha et al., 2025), making these species suitable models for evaluating long-term climate vulnerability.

Handroanthus species exhibit many of the characteristics commonly associated with tropical trees, including long life cycles, ecological dependence on climatic conditions, and vulnerability to environmental change (Almeida et al., 2024; Shang et al., 2025), making them an appropriate case study for evaluating climate-driven distributional shifts.

Within this context, species of the genus *Handroanthus* (Bignoniaceae) provide an appropriate case study for assessing climate-driven distributional changes using an integrated modeling framework. These neotropical tree species are widely distributed across Brazilian phytogeographic domains and have high ecological and socioeconomic importance (Almeida et al., 2024). Brazilian purple ipê (*Handroanthus impetiginosus* (Mart. *ex* DC.) Mattos), and Brazilian yellow ipê (*Handroanthus serratifolius* (Vahl) S.Grose) are valued for their dense and durable wood, but intensive logging, land-use change, and habitat fragmentation have substantially reduced natural populations, increasing their vulnerability to environmental change (Almeida et al., 2024; Shang et al., 2025).

Physiological studies indicate contrasting stress tolerances between these species. *Handroanthus impetiginosus* is more sensitive to abiotic stress during early development, whereas *H. serratifolius* shows greater tolerance to water deficit and low-fertility soils, although both remain vulnerable to climate change (Malecha et al., 2025). Based on these differences, we hypothesize that *H. impetiginosus* will exhibit higher climatic vulnerability and greater reductions in environmentally suitable areas under future climate scenarios than *H. serratifolius*. These contrasting physiological traits provide a mechanistic basis for expecting different responses to climate change, supporting the formulation of our hypothesis.

To test this hypothesis, this study applies an integrated ecological niche modeling framework combining climatic, edaphic, and topographic predictors, PCA-based dimensionality reduction, multiple algorithms, and a performance-weighted consensus approach. This framework allows us to evaluate whether species-specific physiological traits are reflected in contrasting patterns of environmental suitability and climate-driven distribution shifts across Brazilian phytogeographic domains.

Methods

Occurrence data collection and processing. Occurrence records of *Handroanthus impetiginosus* and *Handroanthus serratifolius* were obtained from SpeciesLink (CRIA, 2025), GBIF (2025), and institutional botanical collections (UFAM and INPA). Data curation included the removal of duplicate, incomplete, and geographically inconsistent records, followed by coordinate validation and spatial filtering.

To reduce spatial autocorrelation and sampling bias, which can inflate model performance in large-scale ecological niche models, occurrence records were spatially rarefied using a minimum distance of 5 km between points with the SPThin package (Aiello-Lammens et al., 2015). This procedure resulted in spatially balanced datasets suitable for modeling species distributions across Brazil.

DOI: 10.4206/Bosque.e4709

Environmental predictors and construction of the modeling base. Species distributions were modeled using climatic, edaphic, and topographic variables representing key environmental gradients affecting tropical tree occurrence (Andrade et al., 2020). In total, 33 predictors were considered, including 19 bioclimatic variables from WorldClim v2.1 and 14 edaphic variables from SoilGrids (Fick & Hijmans, 2017; ISRIC, 2025). Climatic predictors were derived from WorldClim v2.1, representing baseline conditions for the period 1970–2000. This baseline was used both for model calibration and as a reference for current environmental suitability, following standard practices in ecological niche modeling. Elevation and slope from EarthEnv were included to capture geomorphological and microclimatic variation (Alvarez et al., 2022). A detailed description of predictors is provided in Table S1.

Dimensionality reduction and environmental gradientes. To summarize correlated environmental predictors and optimize model performance, a PCA was applied to the historical environmental dataset (1970–2000), integrating climatic and edaphic variables. Rather than eliminating collinearity in the original variables, PCA transforms them into orthogonal components that capture the main environmental gradients while reducing dimensionality and redundancy in the predictor set. Components explaining at least 95% of the total variance were retained for modeling (Velazco et al., 2017). The contribution of individual variables to each component was examined to support ecological interpretation of the modeled niches. The complete list of environmental variables, PCA loadings, and variance explained by each component are provided in Tables S1, S2 and S3.

Future climate projections. Future projections were based on CMIP6 climate data from the CNRM-CM6-1 global circulation model, obtained through WorldClim and aligned with the IPCC Sixth Assessment Report (IPCC, 2023). The use of a single General Circultion Model (GCM) allowed standardization of climate projections across scenarios, facilitating a clearer assessment of the effects of predictor selection, dimensionality reduction, and algorithmic variability on model outputs. Although multi-GCM ensembles are commonly recommended to better represent uncertainty in future climate projections and improve the assessment of climate-related risks (Fadda et al., 2026; IPCC, 2023; Xu et al., 2025), the use of a single GCM in this study enabled a more controlled evaluation of methodological uncertainty associated with the ecological niche modeling framework.

Three future periods were considered (2041–2060, 2061–2080, and 2081–2100) under two emission scenarios: SSP2-4.5, representing an intermediate mitigation pathway, and SSP5-8.5, representing a high-emission scenario (Alvarez et al., 2022; Magalhães et al., 2025; Velazco et al., 2017). These scenarios were used to evaluate the stability, contraction, or displacement of environmentally suitable areas throughout the 21st century.

Ecological niche modeling and consensus projections. Ecological niche models were developed using the ENMTML package (Ecological Niche Modelling at The MetaLand EcologyLab), which allows multi-algorithm modeling within a standardized framework (Andrade et al., 2020). Six algorithms were selected based on predictive performance (Magalhães et al., 2025; Morais et al., 2025). Pseudo-absences (1,000 per algorithm) were generated within the accessible area (M), defined as the geographic extent of Brazil, encompassing all phytogeographic domains where the species are known to occur. This delimitation represents the environmentally accessible region at the spatial scale considered and follows the conceptual framework of Barve et al. (2011).

Model performance was assessed using AUC (Area Under the Curve), with values ≥ 0.7 considered acceptable (Jiménez-Valverde, 2012), and only consistently performing models were retained. Final distribution maps were produced through an AUC-weighted ensemble approach (Marmion et al., 2009). Continuous outputs were converted to binary maps using the Maximum True Skill Statistic threshold (MX_TSS) (Allouche et al., 2006), and environmentally suitable areas (km²) were quantified in R to evaluate climate vulnerability across Brazilian phytogeographic domains. Additional performance metrics are provided in Table S4.

Results

Occurrence points of the species studied. A total of 4,130 occurrence records were compiled (1,930 for *Handroanthus impetiginosus* and 2,200 for *Handroanthus serratifolius*). After data cleaning and spatial filtering, the final dataset comprised 805 and 638 records per species, respectively. Geographic distribution patterns differ between species. *H. impetiginosus* presents greater density and amplitude of occurrence, with predominance in the Atlantic Forest, Cerrado, and Caatinga, as well as records in the Pantanal, Pampa, and specific areas of the Amazon. In contrast, *H. serratifolius* displays a more heterogeneous distribution; although widely present in Brazilian domains, it is most often found in the Cerrado, Atlantic Forest, and Caatinga, and in sparse occurrences in the Amazon, Pantanal, and Pampa (Figure 1).

DOI: 10.4206/Bosque.e4709

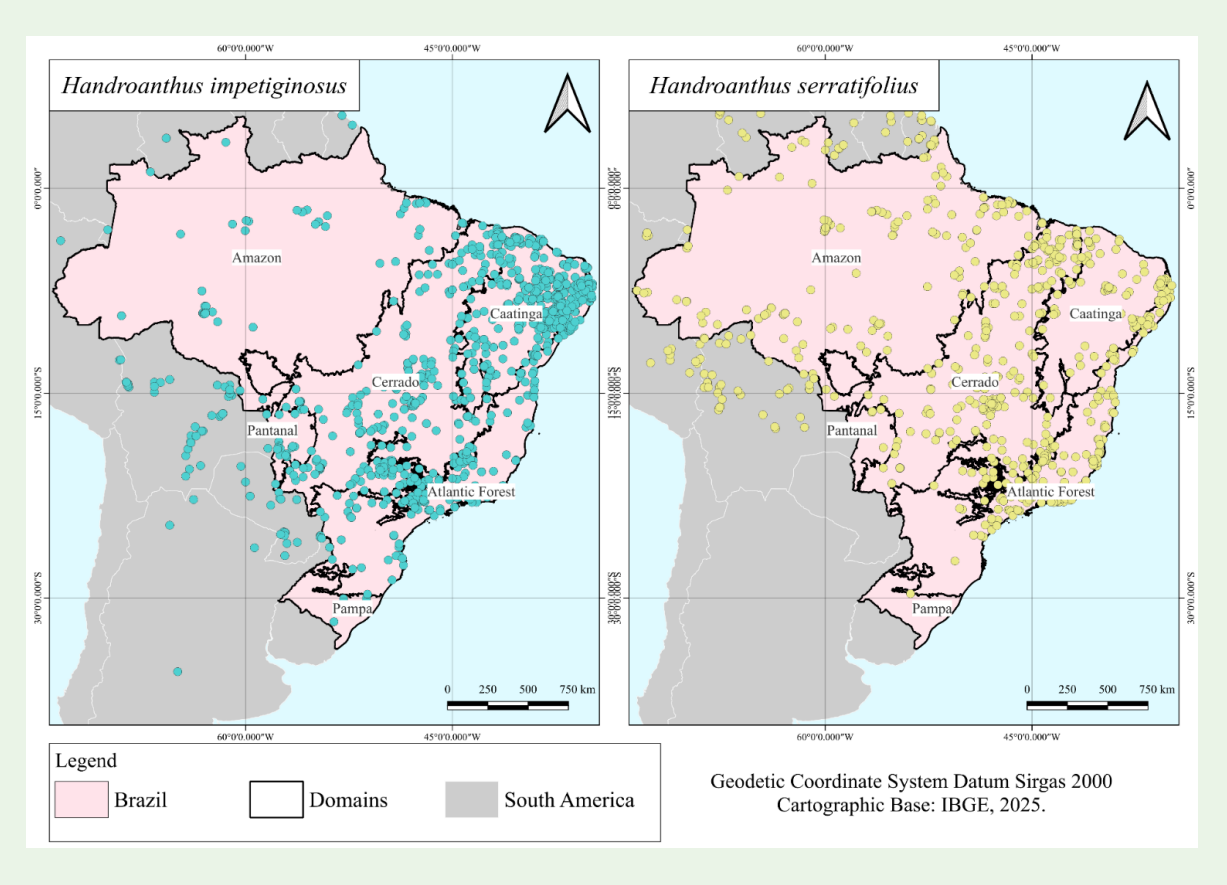

Figure 1. Geographic distribution of *H. impetiginosus* and *H. serratifolius* in South America after collinearity analysis and spatial reduction. Source: Author (2025).

The accessible area (M) used for model calibration was defined as the geographic extent of Brazil, encompassing all phytogeographic domains where the species are known to occur. This delimitation reflects the broad distribution of *Handroanthus impetiginosus* and *H. serratifolius* and represents the environmentally accessible region at the spatial scale considered in this study, following the conceptual framework proposed by Barve et al. (2011).

Environmental variables. The PCA revealed that environmental variation is primarily structured by edaphic, climatic, and topographic variables. A total of 13 principal components (PC1–PC13) were retained, explaining more than 95.85% of the total environmental variance (Table 1). The first components accounted for the largest proportion of variance, with a gradual decrease in explanatory power across subsequent components, indicating effective dimensionality reduction (Table S2).

The highest loadings were associated with soil attributes related to texture (silt, clay, and sand), bulk density, and organic carbon, highlighting the importance of soil physical and chemical properties for water availability and species establishment (Table 1). Cation exchange capacity and the proportion of coarse fragments also showed strong contributions, reinforcing the role of substrate characteristics in defining the ecological niche. Climatic variables, including temperature range, isothermality, and precipitation seasonality, together with slope, were also identified as important drivers of species distribution patterns (Table 1). The full PCA rotation matrix (loadings) is provided in Table S3.

Validation of the models. Performance evaluations of the algorithms revealed similar patterns for both species. In *H. impetiginosus*, the Random Forest presented the best performance, with an AUC of 0.988 ± 0.003, followed by Bayesian Gaussian Process (GAU) and Support Vector Machine (SVM) (both with 0.982 ± 0.004), showing high efficiency in the distinction between suitable and unsuitable areas. All evaluation metrics consistently identified Random Forest as the best-performing algorithm (Table 2). For *H. serratifolius*, an

DOI: 10.4206/Bosque.e4709

Table 1. Main environmental variables and their weights (eigenvectors) in the first 13 principal components (PC1–PC13) determining the distribution and ecological niche of *H. impetiginosus* and *H. serratifolius*.

Main Components	Variables	Eigenvector	Variables	Eigenvector	Variables	Eigenvector
PC1	BIO06	0.26304	BIO11	0.25867	BIO01	0.25012
PC2	ocs30	0.32438	ocd30	0.32049	nitrogen30	0.31202
PC3	BIO15	0.35342	BIO04	–0.31267	Elevação	0.31152
PC4	sand30	–0.54419	silt30	0.48227	clay30	0.34865
PC5	BIO18	–0.48316	BIO02	–0.40139	Elevação	–0.34067
PC6	cfvo30	0.33847	BIO14	0.28643	WRB	0.28379
PC7	clay30	0.53855	BIO18	–0.41646	bio150	–0.30215
PC8	BIO19	–0.54508	WRB	0.41460	BIO13	–0.25857
PC9	WRB	0.77850	silt30	–0.35029	clay30	0.24320
PC10	slope1	0.75503	BIO05	–0.26614	BIO10	0.21701
PC11	clay30	–0.51077	soc30	–0.40917	silt30	0.32117
PC12	BIO02	–0.46899	cec30	–0.39521	BIO03	–0.35366
PC13	bdod30	0.77005	soc30	–0.33514	ocs30	0.23024

Bio1–Bio11: thermal variables; Bio12–Bio19: precipitation variables. Edaphic and topographic variables: elevation, slope1, pH (0–30 cm), texture (sand30, silt30, clay30), bulk density (bdod30), soil organic carbon (soc30, ocd30, ocs30), total nitrogen (nitrogen30), cation exchange capacity (cec30), coarse fragments (cfvo30), and WRB soil classes.

equivalent pattern was observed, with the Random Forest again standing out in all metrics analyzed. The algorithm achieved an AUC of 0.989 ± 0.003, as well as high values of Kappa and TSS (0.904 ± 0.014), as well as Jaccard indices (0.909 ± 0.013) and Sorensen (0.952 ± 0.007), confirming its superiority in the representation of the spatial pattern of species distribution (Table 2).

Projection of environmental suitability. Based on baseline (1970–2000) environmental suitability maps, which represent current conditions in the modeling framework, *H. impetiginosus* shows high current suitability in the Atlantic Forest and central to southern regions of the Cerrado and Caatinga, whereas most of the Amazon, Pampa, and Pantanal exhibit low suitability (Figure 2). *H. serratifolius* presents a similar pattern, with higher suitability in the Atlantic Forest and southern Cerrado and reduced suitability across large portions of the Amazon, Caatinga, and Pantanal (Figure 2).

Future projections indicate marked reductions in environmental suitability for *H. impetiginosus*, particularly under the SSP5-8.5 scenario, with progressive contraction of suitable areas and near collapse by the end of the century (Figure 3). In contrast, *H. serratifolius* maintains broader suitability under SSP2-4.5, with gradual reductions over time, while under SSP5-8.5 suitability becomes increasingly restricted to warmer and seasonally dry regions of the Northeast and interior portions of the Center-West and Southeast, indicating a shift toward hotter and drier climatic conditions (Figure 4).

Handroanthus impetiginosus. In the SSP2-4.5 scenario, there are strong reductions of environmental adequacy in all domains, above 65% in the Amazon by 2041-2060 and above 80% by 2100, with almost total collapse in the Pampa and Pantanal (Table 3). In the SSP5-8.5 scenario, losses are almost total, exceeding 99% in the Amazon and occurring early in the Pantanal and Pampa, resulting in a reduction of 81% of the adequate area already in 2041-2060 and 98.6% by the end of the century, which shows the species' high vulnerability to climate change.

DOI: 10.4206/Bosque.e4709

Table 2. Performance of ecological niche modeling algorithms for *H. impetiginosus* and *H. serratifolius* evaluated by AUC, Kappa, TSS, Jaccard, and Sorensen metrics (mean ± standard deviation).

Handroanthus impetiginosus					
Algorithms	Metrics				
	AUC[7]	Kappa	TSS[8]	Jaccard	Sorensen
BIO[1]	0.976 ± 0.010	0.901±0.033	0.901±0.033	0.903±0.320	0.948±0.017
GAU[2]	0.982±0.004	0.893 ±0.012	0.893 ±0.012	0.900±0.011	0.947±0.006
GLM[3]	0.977±0.006	0.888 ±0.014	0.888 ±0.014	0.894±0.014	0.944±0.007
MXD[4]	0.966±0.004	0.838 ±0.025	0.838 ±0.025	0.851±0.023	0.919±0.013
RDF[5]	0.988±0.003	0.910 ±0.011	0.910 ±0.011	0.914±0.011	0.955±0.006
SVM[6]	0.982±0.004	0.901 ±0.013	0.901 ±0.013	0.907±0.012	0.951±0.006
Handroanthus serratifolius					
Algorithms	Metrics				
	AUC[7]	Kappa	TSS[8]	Jaccard	Sorensen
BIO[1]	0.977±0.010	0.931±0.027	0.931±0.027	0.931±0.027	0.964±0.014
GAU[2]	0.986±0.002	0.890±0.014	0.890±0.014	0.898±0.014	0.946±0.008
GLM[3]	0.978±0.003	0.894±0.018	0.894±0.018	0.899±0.017	0.947±0.009
MXD[4]	0.969±0.004	0.860±0.014	0.860±0.014	0.873±0.013	0.932±0.007
RDF[5]	0.989±0.003	0.904±0.014	0.904±0.014	0.909±0.013	0.952±0.007
SVM[6]	0.984±0.003	0.887±0.016	0.887±0.016	0.894±0.014	0.944±0.008

[1] BIO = Bioclim; [2] GAU = Bayesian Gaussian Process; [3] GLM = [4] MXD = Maximum Entropy Default; [5] RDF = Random Forests; [6] SVM = Support Vector Machine; [7] AUC = Area Under the Curve; [8] TSS = True Skill Statistics.

Handroanthus serratifolius. *H. serratifolius* presents greater stability of environmentally suitable areas in future scenarios, maintaining a large proportion of its potential distribution even under more severe climatic conditions (Table 3). In the SSP2-4.5 scenario, the species retains much of its suitability in the Amazon (75-78%), while Cerrado, Caatinga, and Mata Atlântica show moderate reductions over the century, resulting in a total loss of about 19-21% of the potential area (Table 3). Already in the most extreme scenario (SSP5-8.5) and considering there are more pronounced reductions projected at the end of the century, especially in the Caatinga and Pantanal, the species maintains high levels of suitability in the Amazon, Cerrado, and Atlantic Forest. In all domains, losses reached approximately 38% by 2100, indicating greater climatic tolerance of *H. serratifolius* compared to *H. impetiginosus*.

Discussion

The ecological niche modeling framework applied in this study revealed a consistent pattern of progressive reduction in environmentally suitable areas throughout the 21st century, particularly under the SSP5-8.5 scenario. By integrating climatic, edaphic, and topographic predictors within a consensus-based approach, the models were able to identify regions where increases in temperature, reductions in humidity, and intensified climatic extremes impose strong constraints on species persistence. The most pronounced losses were projected for the Caatinga, Cerrado, and Pantanal, a pattern commonly detected by large-scale models applied to tropical trees associated with seasonal environments (Aragão & Groenendijk, 2025). These results reinforce the capacity of the modeling framework to capture climate-driven vulnerability gradients across heterogeneous landscapes.

DOI: 10.4206/Bosque.e4709

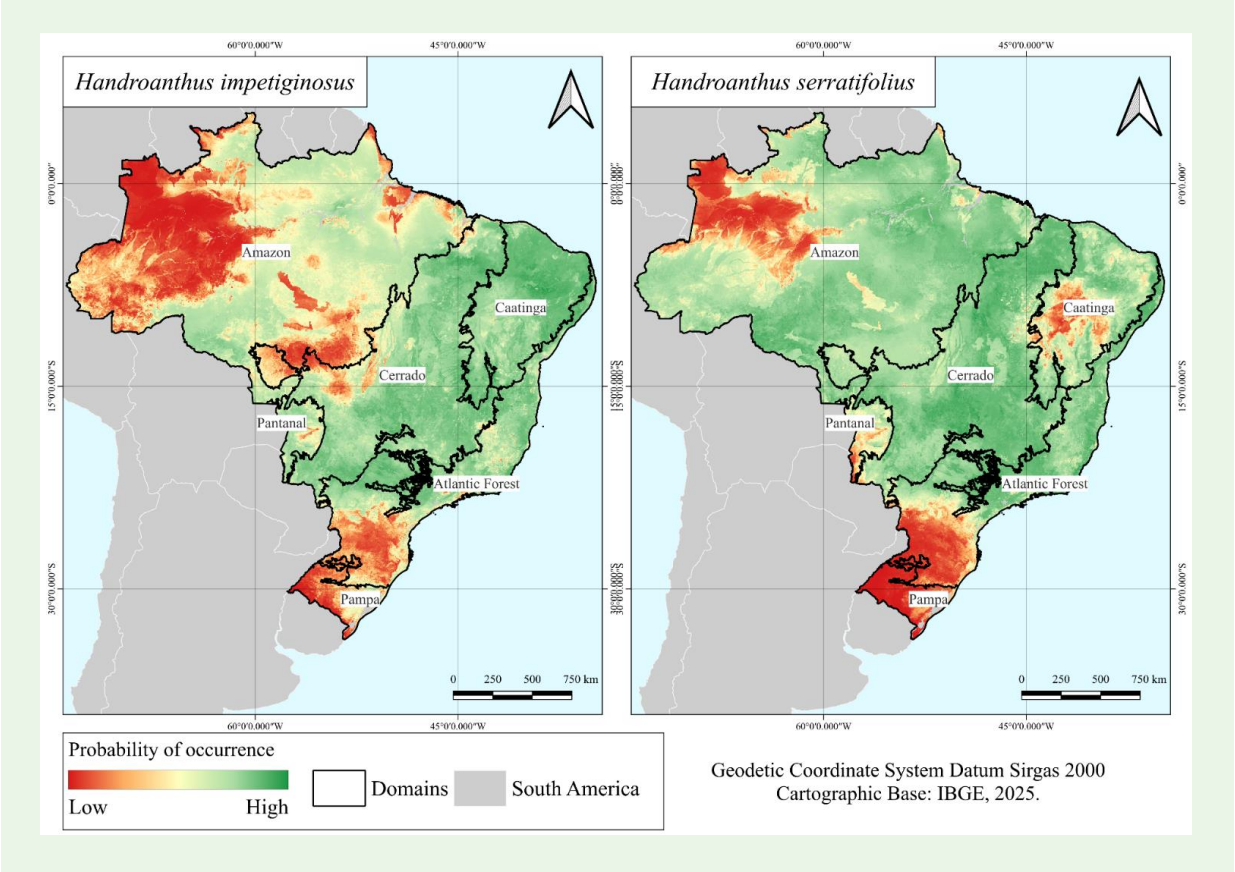

Figure 2. Projection of current environmental suitability based on baseline climate conditions (1970–2000) of *H. impetiginosus* and *H. serratifolius*. Source: Author (2025).

Using *Handroanthus impetiginosus* and *Handroanthus serratifolius* as a case study, the modeled patterns are consistent with known ecological and functional attributes of the genus. Species of the family Bignoniaceae have high ecological, ornamental, and timber value and are widely used in urban landscaping due to the density and durability of their wood (Shang et al., 2025). Although anatomical adaptations to seasonal environments, such as thick cuticles and anomocytic stomata, may confer some tolerance, these traits appear insufficient to offset the magnitude of climatic stress projected by the models, particularly under high-emission scenarios (Oliveira et al., 2025). Similar responses have been reported for other economically valuable genera subjected to combined pressures of exploitation and habitat restriction, highlighting the relevance of modeling approaches for informing sustainable management strategies (Carvalho et al., 2025).

The spatial patterns identified by the models are further supported by complementary evidence from environmental zoning and plant physiological studies, which indicate that species of the genus *Handroanthus* depend on climatic regimes characterized by relatively stable water availability (Martorano et al.,2025). Experimental studies show that *H. impetiginosus* exhibits moderate resistance to water deficit but high sensitivity to salinity, resulting in reduced growth, biomass accumulation, and photosynthetic efficiency (Moura et al., 2025). Additionally, heavy metal contamination represents an important risk factor, as mercury accumulation in plant tissues can induce oxidative stress and impair photosynthetic performance (Oliveira et al., 2025). These physiological constraints are coherent with the reductions in environmental suitability projected by the modeling framework.

Limitations related to natural regeneration also emerge as a critical component of climate vulnerability. Differences in seed physiological behavior combined with slow initial seedling growth increase susceptibility to thermal variability and climatic extremes, particularly in fragmented landscapes. Comparable reductions in suitable areas have been reported for other widely distributed tropical tree species under future climate scenarios (Marques et al., 2024;

DOI: 10.4206/Bosque.e4709

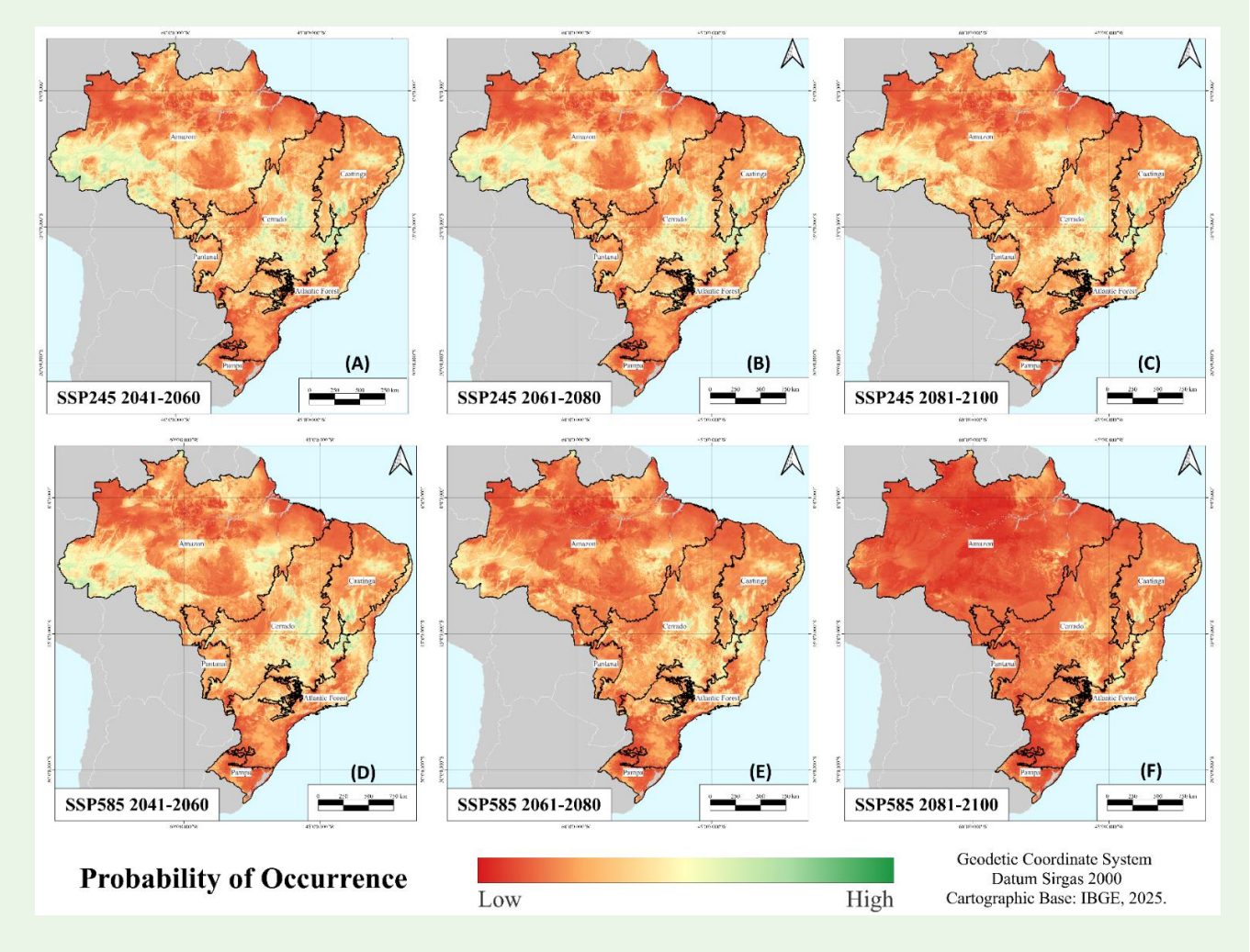

Figure 3. Projection of environmental suitability of *Handroanthus impetiginosus* under SSP2-4.5 (A–C) and SSP5-8.5 (D–F) scenarios for 2041–2060, 2061–2080, and 2081–2100 in Brazilian phytogeographic domains. Source: Author (2025).

Santos et al., 2025). These convergent patterns reinforce the broader applicability of the modeling framework beyond the focal species.

While the modeling framework provides consistent and reliable projections, some limitations should be acknowledged. Future projections were based on a single global circulation model (CNRM-CM6-1), which may not fully capture the range of variability among climate models. Multi-model ensembles are widely recommended to better represent this uncertainty. However, the use of a single GCM allowed the standardization of climate inputs and facilitated a clearer evaluation of uncertainty associated with the ecological niche modeling framework itself. Therefore, projected suitability patterns should be interpreted within this scope, and future studies incorporating multiple GCMs may further refine climate vulnerability assessments.

Beyond projected spatial losses, habitat contraction and isolation identified by the models may compromise genetic connectivity, reducing gene flow and adaptive potential over time (Santos et al., 2025). For Brazilian ipês, historically subjected to selective exploitation, these processes pose significant challenges for forest management, ecological restoration, and seed production. In this context, the integration of ecological niche modeling with sustainable forest management, *ex situ* conservation strategies, topoclimatic zoning, and continuous monitoring of abiotic stressors emerges as a critical approach to mitigate climate change impacts, particularly in regions identified as highly vulnerable by the modeling framework (Aragão & Groenendijk, 2025).

DOI: 10.4206/Bosque.e4709

Table 3. Projections of gain (+) or loss (−) of environmental suitability (%) under SSP2-4.5 and SSP5-8.5 scenarios relative to the current period for *H. impetiginosus* and *H. serratifolius* in Brazilian phytogeographic domains.

H. impetiginosus				
		SSP2-4.5		
Domain	Current (km²)	2041-2060	2061-2080	2081-2100
Amazon	2,319,039.39	809,426.10	691,882.60	433,681.53
Caatinga	880,654.73	101,064.43	89,919.37	73,266.83
Cerrado	1,894,920.06	446,994.89	350,874.18	303,778.72
Atlantic Forest	870,485.41	96,662.78	100,825.91	73,050.00
Pampa	39,571.46	0.00	0.00	0.00
Pantanal	146,620.39	932.37	325.24	130.10
Total	6,151,291.44	1,455,080.56	1,233,827.31	883,907.18
		SSP5-8.5		
Amazon	2,319,039.39	596,585.85	127,018.97	4,293.23
Caatinga	880,654.73	84,737.13	51,236.91	18,322.13
Cerrado	1,894,920.06	374,096.67	175,870.75	37,208.01
Atlantic Forest	870,485.41	88,705.12	61,276.14	26,800.18
Pampa	39,571.46	0.00	0.00	0.00
Pantanal	146,620.39	325.24	17.03	0.00
Total	6,151,291.44	1,144,450.01	415,419.80	86,623.55
H. serratifolious				
		SSP2-4.5		
Domain	Current (km²)	2041-2060	2061-2080	2081-2100
Amazon	3,500,675.73	2,721,475.72	2,754,563.97	2,641,725.68
Caatinga	666,752.01	389,925.25	383,702.23	344,022.36
Cerrado	2,047,741.79	1,950,190.01	1,938,025.85	1,925,840.01
Atlantic Forest	823,216.48	613,932.24	633,772.18	627,007.09
Pampa	151.78	0.00	0.00	0.00
Pantanal	93,583.79	87,512.56	84,845.55	72,984.95
Total	7,132,121.59	5,763,035.78	5,794,909.78	5,611,580.08
		SSP5-8.5		
Amazon	3,500,675.73	2,695,000.79	2,636,868.69	1,929,070.77
Caatinga	666,752.01	372,513.81	304,234.06	191,417.46
Cerrado	2,047,741.79	1,945,072.82	1,894,941.74	1,703,545.97
Atlantic Forest	823,216.48	623,342.66	628,438.16	574,534.25
Pampa	151.78	0.00	0.00	0.00
Pantanal	93,583.79	82,980.81	60,690.70	39,202.85
Total	7,132,121.59	5,718,910.89	5,525,173.35	4,437,771.29

DOI: 10.4206/Bosque.e4709

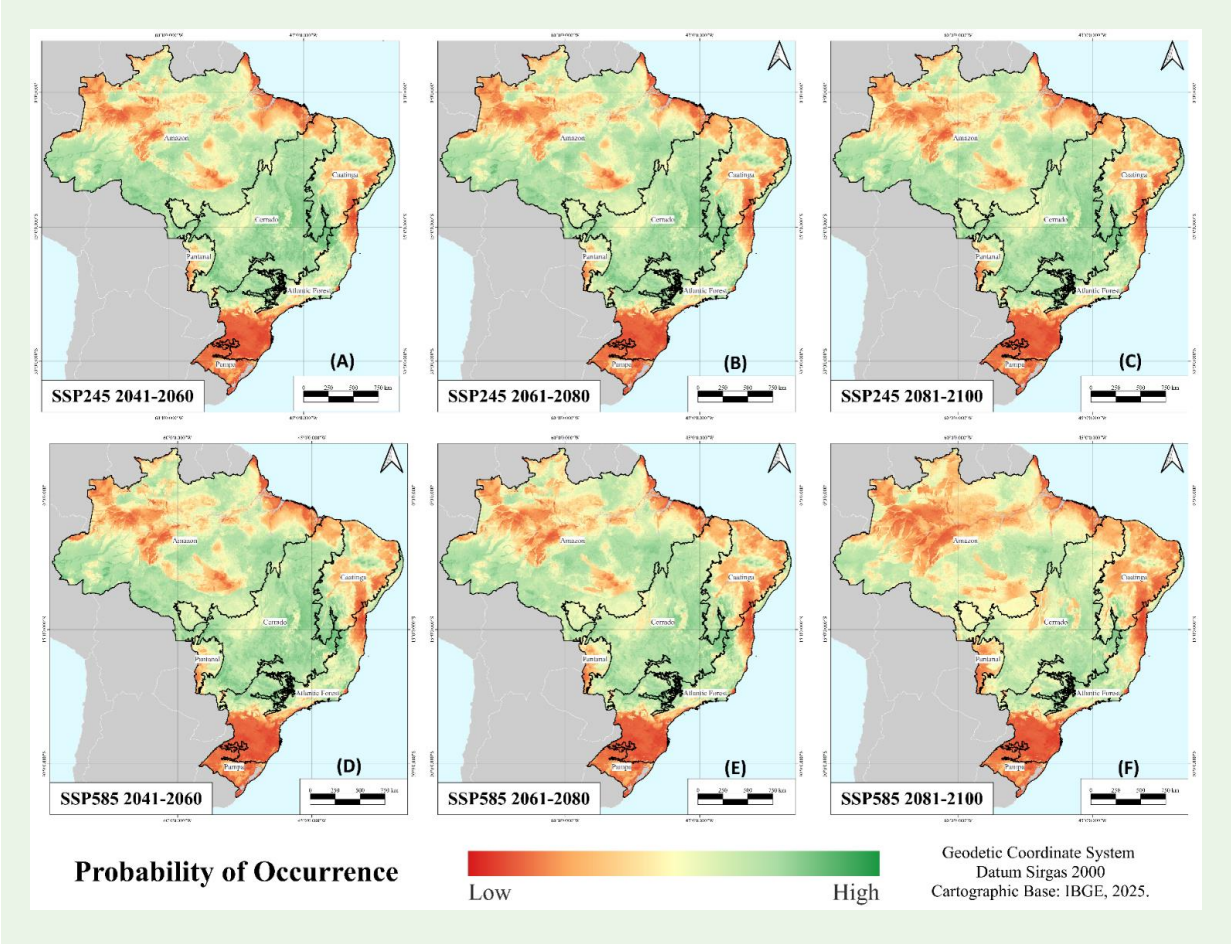

Figure 4. Projection of environmental suitability of *Handroanthus serratifolius* under SSP2-4.5 (A–C) and SSP5-8.5 (D–F) scenarios for 2041–2060, 2061–2080, and 2081–2100 in Brazilian phytogeographic domains. Source: Author (2025).

Conclusion

This study demonstrates the effectiveness of an integrated ecological niche modeling framework to assess climate vulnerability and future distribution patterns of tropical tree species at broad spatial scales. By combining climatic, edaphic, and topographic predictors with dimensionality reduction, multi-algorithm modeling, and consensus-based projections, the framework captured patterns of environmental stability and loss under contrasting climate scenarios. Applied to *Handroanthus impetiginosus* and *H. serratifolius*, the results revealed contrasting responses, with higher vulnerability projected for *H. impetiginosus* and greater climatic tolerance for *H. serratifolius*. Overall, the framework provides a transferable tool to support climate-informed conservation planning and sustainable forest management under future climate change.

Authors contributions

All authors contributed to the study conception and design; F.C.B., C.S.B., J.S.T., M.J.M. and H.L.V.C. collected the data; S.F.S. and S.L.F.R. performed the data analyses; all authors interpreted the results; F.C.B., C.S.B., J.S.T., R.L., C.H.S.G.G.M. and M.T.G.L; wrote the first draft of the manuscript; all authors re-viewed and edited the manuscript; all authors read and approved the final manuscript.

Funding

This study was funded by the Coordination for the Improvement of Higher Education Personnel (CAPES; Call no. 16/2020 – PROCAD-SPCF, Process no. 88881.516217/2020-01) and the Graduate Development Program – Strategic Postdoctoral Program (CAPES-PDPG; Call no. 16/2022, Process no. 88887.692247/2022-00).

Acknowledgements

The authors acknowledge the Coordination for the Improvement of Higher Education Personnel (CAPES; Call no. 16/2020 – PROCAD-SPCF, Process no. 88881.516217/2020-01) and the National Council for Scientific and Technological Development (CNPq) for research productivity grants awarded to C.H.S.G.M. (306943/2025-5), S.L.F.R. (305280/2022-8), R.L. (308815/2023-8), and M.T.G.L. (306943/2025-5).

AI use declaration

The authors used ChatGPT (OpenAI, GPT-5.5) solely as a support tool for identifying and correcting English language errors and for assisting with the formatting of references in the final stages of manuscript preparation. The AI tool was not used for study design, data collection, data analysis, interpretation of results, or generation of scientific content. All suggestions provided by the AI were carefully reviewed, verified, and edited by the authors, who take full responsibility for the accuracy and integrity of the manuscript.

References

Aiello-Lammens, M. E., Boria, R. A., Radosavljevic, A., Vilela, B., & Anderson, R. P. (2015). SpThin: An R package for spatial thinning of species occurrence records for use in ecological niche models. *Ecography, 38*(5), 541–545. DOI: https://doi.org/10.1111/ecog.01132

Allouche, O., Tsoar, A., & Kadmon, R. (2006). Assessing the accuracy of species distribution models: prevalence, kappa and the true skill statistic (TSS). *Journal of Applied Ecology*, *43*(6), 1223–1232. DOI: https://doi.org/10.1111/j.1365-2664.2006.01214.x

Almeida, R. S., Araújo, J. K. P., Araújo, M. P., Moura, L. B., Gomes, A. C., Barbosa, F. M., & Lacerda, A. V. (2024). Biometria de sementes de *Handroanthus impetiginosus* e produção de mudas após diferentes períodos de imersão em água. *Pesquisa Agropecuária Brasileira*, *59*, e03568. DOI: https://doi.org/10.1590/S1678-3921.pab2024.v59.03568

Alvarez, F., Morandi, P. S., Marimon-Junior, B. H., Exavier, R., Araújo, I., Mariano, L. H., Muller, A. O., Felpausch, T. R., & Marimon, B. S. (2022). Climate defined but not soil-restricted: the distribution of a Neotropical tree through space and time. *Plant and Soil, 471*, 175–191. DOI: https://doi.org/10.1007/s11104-021-05202-6

Andrade, A. F. A., Velazco, S. J. E., & Marco Júnior, P. (2020). ENMTML: An R package for a straightforward construction of complex ecological niche models. *Environmental Modelling & Software, 125*, 104615. DOI: https://doi.org/10.1016/j.envsoft.2019.104615

Aragão, J. R. V., & Groenendijk, P. (2025). Tree-ring based growth modelling to aid timber management of congeneric *Aspidosperma* and *Handroanthus* species along a seasonal tropical forest gradient. *Dendrochronologia, 92*, 126377. DOI: https://doi.org/10.1016/j.dendro.2025.126377

Barve, N., Barve, V., Jiménez-Valverde, A., Lira-Noriega, A., Maher, S. P., Peterson, A. T., Soberón, J., & Villalobos, F. (2011). The crucial role of the accessible area in ecological niche modeling and species distribution modeling. *Ecological Modelling*, *222*(11), 1810–1819. DOI: https://doi.org/10.1016/j.ecolmodel.2011.02.011

Bauman, D., Fortunel, C., Cernusak, L. A., Bentley, L. P., McMahon, S. M., Rifai, S. W., Aguirre-Gutiérrez, J., Oliveras, I., Bradford, M., Laurance, S. G. W., Hutchinson, M. F., Dempsey, R., Santos-Andrade, P. E., Ninantay-Rivera, H. R., Chambi Paucar, J. R., & Malhi, Y. (2022). Tropical tree growth sensitivity to climate is driven by species intrinsic growth rate and leaf traits. *Global Change Biology*, *28*(4), 1414–1432. DOI: https://doi.org/10.1111/gcb.15982

Carvalho, C. S., Machado, R. M., Lemes, M. R., & Cardoso, D. (2025). Ecological Niche Modeling Predicts Alarming Impacts of Global Climate Change on Economically Important Neotropical Trees. *Ecology and Evolution*, *15*(9), e72105, 2025. DOI: https://doi.org/10.1002/ece3.72105

Centro de Referência em Informação Ambiental — CRIA (2025). Projeto speciesLink network. http://splink.cria.org.br (Accessed: April 19, 2025).

Fadda, L. A., Lasa-Covarrubias, R., Osorio-Olvera, L., Murúa, M. G., & Lira-Noriega, A. (2026). Applications of ecological niche and species distribution models in agricultural, livestock, and forestry systems: A comprehensive review. *Agricultural Systems*, *231*, 104542. DOI: https://doi.org/10.1016/j.agsy.2025.104542

Fick, S. E., & Hijmans, R. J. (2017). WorldClim 2: New 1 km spatial resolution climate surfaces for global land areas. *International Journal of Climatology*, *37*(12), 4302–4315. DOI: https://doi.org/10.1002/joc.5086

GBIF.org (10 March 2025) GBIF Occurrence Download https://doi.org/10.15468/dl.ak4jkf

Intergovernmental Panel on Climate Change (IPCC) (2023). *Climate change: the physical science basis.* https://www.ipcc.ch/report/ar6/wg1/. (Accessed: January 20, 2025).

Jiménez-Valverde, A. (2012). Insights into the area under the receiver operating characteristic curve (AUC) as a discrimination measure in species distribution modeling. *Global Ecology and Biogeography*, *21*(4), 498–507. DOI: https://doi.org/10.1111/j.1466-8238.2011.00683.x

Magalhães, L. L., Tomaz, J. S., Bezerra, C. S., Lopes, M. T. G., Lopes, R., Souza, S. F., Meneses, C. H. S. G., Aguiar, A. V., Capucho, H. L. V., & Ramos, S. L. F. (2025). Climate Change Threatens the Geographic Distribution of Cupuaçu More Than Cacao: Insights from Ecological Modeling in Brazil. *Ethnobiology and Conservation*, *14*(31), 1–18. DOI: https://doi.org/10.15451/ec2025-09-14.31-1-18

Malecha, A., Manes, S., & Vale, M. M. (2025). Climate change and biodiversity in Brazil: what we know, what we don't, and Paris Agreement's risk reduction potential. *Perspectives in Ecology and Conservation*, *23*(2), 77–84. DOI: https://doi.org/10.1016/j.pecon.2025.03.004

Marmion, M., Parviainen, M., Luoto, M., Heikkinen, R. K., & Thuiller, W. (2009). Evaluation of consensus methods in predictive species distribution modelling. *Diversity and Distributions, 15*(1), 59–69. DOI: https://doi.org/10.1111/j.1472-4642.2008.00491.x

Marques, M. J., Bezerra, C. S., Tomaz, J. S., Lopes, R., Wrege, M. S., Aguiar, A. V., Ramos, S. L. F., Meneses, C. H. S. G., Fraxe, T. J. P., & Lopes, M. T. G. (2024). Predição de distribuição geográfica e modelagem de nicho ecológico de açaizeiros na Amazônia. *Pesquisa Agropecuária Tropical, 54*, e78108. DOI: https://revistas.ufg.br/pat/article/view/78108

Martorano, L. G., Brienza Junior, S., Moraes, J. R. D. S. C. D., Nascimento, W., Lisboa, L. S. S., Correa, D. L., Santos, T. M., Lima, R. F., Magalhães, K. R. S., & Dias, C. T. D. S. (2025). Topoclimatic Zoning in the Brazilian Amazon: Enhancing Sustainability and Resilience of Native Forests in the Face of Climate Change. *Forests*, *16*(6), 1015. DOI: https://doi.org/10.3390/f16061015

Moura, M. B. M. D., Barros, T. F., Silva, T. G. F. D., Santos, W. M. D., Martins, L. D. C. D. S., Silva, E. F. D., Lima, J. M. P. D., Tang, X., Jardim, A. M. D. R. F., Souza, C. A. A. D., Souza, K. R. S., & Souza, L. S. B. D. (2025). Saline Water Stress in Caatinga Species with Potential for Reforestation in the Face of Advancing Desertification in the Brazilian Semiarid Region. *Environments, 12*(7), 239. DOI: https://doi.org/10.3390/environments12070239

Oliveira, E. A., Borella, D. R., Lopes, V. J. S., Battirola, L. D., Andrade, R. L. T. D., & Silva, A. C. D. (2025). Physiological Effects of Mercury on *Handroanthus impetiginosus* (Ipê Roxo) Plants. *Agronomy*, *15*(3), 736. DOI: https://doi.org/10.3390/agronomy15030736

R Core Team, (2024). *R: A language and environment for statistical computing. Free software environment for statistical computing and graphics.* R Foundation for Statistical Computing, Vienna, Austria. https://www.R-project.org/ (Accessed: July 14, 2025)

Santos, P. V. D. S., Lima Junior, M. D. J. V., Souza, S. F. D., Tomaz, J. S., Bezerra, C. D. S., & Lopes, M. T. G. (2025). Predicting Species Distribution and Conserving Rosewood Tree Under Global Climate Change Scenarios. *Floresta e Ambiente*, *32*(3), e20250008. DOI: https://doi.org/10.1590/2179-8087-FLORAM-2025-0008

Shang, X., Wu, Z., Zhang, G., Wang, Y., Li, X., & Zhang, P. (2025). Population structure, genetic diversity and genome-wide association analysis of the seed morphology traits in *Handroanthus chrysanthus* **(**Jacq.) s.o.grose. *BMC Plant Biology*, *25*(1249), 1–15. DOI: https://doi.org/10.1186/s12870-025-07285-0

Thuiller, W. (2024). Ecological niche modelling. *Current Biology, 34*(6), PR225–R229. DOI: https://doi.org/10.1016/j.cub.2024.02.018

Velazco, S. J. E., Galvão, F., Villalobos, F., & Marco Júnior, P. D. (2017). Using worldwide edaphic data to model plant species niches: An assessment at a continental extent. *PLoS ONE, 12*(10), e0186025. DOI: https://journals.plos.org/plosone/article?id=10.1371/journal.pone.0186025

World Soil Information – ISRIC (2025). *SoilGrids: global gridded soil information.* https://www.isric.org/explore/soilgrids. (Accessed: March 10, 2025).

Xu, W., Luo, D., Peterson, K., Zhao, Y., Yu, Y., Ye, Z., Sun, J., Yan, K., & Wang, T. (2025). Advancements in ecological niche models for forest adaptation to climate change: a comprehensive review. *Biological Reviews*, *100*, 1754–1781. DOI: https://doi.org/10.1111/brv.70023

DOI: 10.4206/Bosque.e4709

Supporting information

Table S1. Environmental predictors used in the ecological niche modeling framework. Climatic variables derived from WorldClim v2.1 (1970–2000) were used to characterize temperature and precipitation gradients, while edaphic variables obtained from SoilGrids represent soil texture, chemical properties, and structural attributes. Topographic variables (elevation and slope) were included to account for geomorphological constraints on species distribution.

Code	Variable	Unit of measurement
Bio1	Average annual temperature	°C
Bio2	Monthly average of daily temperature variation (temp. maximum - temp. minimum)	°C
Bio3	Isothermality (Bioc2/Bioc7) (* 100)	%
Bio4	Temperature seasonality (standard deviation *100)	%
Bio5	Maximum temperature in the hottest month	°C
Bio6	Minimum temperature in the coldest month	°C
Bio7	Annual temperature variation (Bioc5-Bioc6)	°C
Bio8	Average temperature in the wettest quarter	°C
Bio9	Average temperature in the driest quarter	°C
Bio10	Average temperature in the hottest quarter	°C
Bio11	Average temperature in the coldest quarter	°C
Bio12	Rainfall accumulated in the year	mm
Bio13	Accumulated rainfall in the wettest month	mm
Bio14	Accumulated rainfall in the driest month	mm
Bio15	Seasonality of rainfall (coefficient of variation)	mm
Bio16	Rainfall accumulated in the wettest quarter	mm
Bio17	Accumulated rainfall in the driest quarter	mm
Bio18	Accumulated rainfall in the hottest quarter	mm
Bio19	Accumulated rainfall in the coldest quarter	mm
Slope	Slope	m
Elevation	Elevation	m
Bdod	Apparent density	cg cm^{-3}
Cec	Cation exchange capacity at pH 7	mmol(c) kg^{-1}
Cfvo	Volumetric thick fragments	cm^3 dm^{-3}
Clay	Clay	g kg^{-1}
Nitrogen	Nitrogen	cg kg^{-1}
Ocd	Densities of organic carbon	hg m^{-3}
Ocs	Stock of organic soil carbon	t ha^{-1}
phh20	PH of soil in H2O	pH*10
Sand	Sand	g kg^{-1}
Silt	Silte	g kg^{-1}
Soc	Organic carbon content of soil	dg kg^{-1}
Wrb	Classes and probabilities “World Reference Base”	-

Source: WorldClim (2023), and International Soil Reference and Information Centre – ISRIC (2024).

DOI: 10.4206/Bosque.e4709

Table S2. Variance explained by principal components derived from climatic, edaphic, and topographic variables used in the ecological niche modeling framework.

PC	Variable Explained (%)	Cumulative Variance (%)
PC1	40.31	40.31
PC2	21.40	61.71
PC3	9.02	70.73
PC4	5.43	76.17
PC5	4.09	80.26
PC6	3.38	83.63
PC7	2.72	86.35
PC8	2.55	88.90
PC9	2.06	90.96
PC10	1.60	92.56
PC11	1.35	93.92
PC12	0.99	94.91
PC13	0.94	95.85

Note: Principal components were retained based on cumulative variance, adopting a threshold ≥ 95%, resulting in the selection of 13 components.

Table S3. Complete PCA rotation matrix (loadings) for all environmental variables across the retained principal components (PC1–PC13). This table provides the full contribution of each predictor variable to each principal component. For clarity, only the most influential variables are presented in the main manuscript (Table 1).

Variable	PC1	PC2	PC3	PC4	PC5	PC6	PC7	PC8	PC9	PC10	PC11	PC12	PC13
bdod30	0.013345	-0.3024	-0.1062	0.096893	-0.011	0.13155	-0.15496	0.108799	-0.14089	0.069177	-0.19732	0.062647	0.770045
bio01	0.250122	-0.13408	-0.02052	0.018882	0.081708	-0.02059	-0.04546	0.12862	-0.00793	0.113625	-0.02341	-0.0591	-0.05824
bio02	-0.16078	-0.18664	0.00703	0.088585	-0.40193	-0.14524	-0.13518	-0.08989	-0.04111	0.18831	-0.08945	-0.4689	-0.16462
bio03	0.198708	0.038392	0.287459	0.075181	-0.11552	0.257289	-0.03016	0.165898	-0.0907	-0.04853	0.114231	-0.3536	-0.10408
bio04	-0.21098	-0.05189	-0.31267	-0.08929	-0.01008	-0.05455	0.007819	-0.18523	0.036191	0.18108	-0.09788	0.149298	-0.02445
bio05	0.188319	-0.22586	-0.16908	-0.01247	0.071348	-0.07955	-0.10782	-0.01921	-0.00114	0.266142	-0.04906	-0.14784	-0.12461
bio06	0.26304	-0.04979	0.04605	0.001898	0.161066	0.069331	-0.01564	0.119587	-0.01403	0.03413	0.027506	-0.02985	-0.02117
bio07	-0.21236	-0.12999	-0.21795	-0.0139	-0.16937	-0.17155	-0.07381	-0.19034	0.019288	0.188697	-0.08372	-0.08905	-0.08083
bio08	0.218576	-0.16375	-0.09236	0.076457	-0.01294	-0.05603	-0.0917	0.206436	-0.05213	0.185985	-0.09847	-0.01921	0.049358
bio09	0.249396	-0.07391	0.069476	-0.03656	0.181198	0.048238	-0.00161	0.033277	0.018133	0.024053	0.042779	-0.08785	-0.13422
bio10	0.219524	-0.17933	-0.15315	-0.01552	0.11083	-0.03544	-0.05592	0.064314	0.001704	0.217011	-0.06048	-0.01767	-0.08007
bio11	0.258607	-0.09202	0.066194	0.038067	0.07605	0.002389	-0.0384	0.14545	-0.01662	0.046239	0.009995	-0.09056	-0.03932
bio12	0.232163	0.152515	-0.01574	-0.07458	-0.17983	-0.00991	-0.14035	-0.16414	0.034515	0.000638	0.011739	0.040154	0.040884
bio13	0.236015	0.083505	0.109995	0.011312	-0.09483	-0.14991	-0.1996	-0.25857	0.091588	-0.03484	-0.03399	0.083475	0.059509
bio14	0.126617	0.226686	-0.18592	-0.20823	-0.26758	0.286434	0.031676	0.069554	-0.05238	0.116878	-0.09589	-0.03833	0.084631
bio15	-0.03757	-0.17633	0.353419	0.252276	-0.01363	-0.22425	-0.30251	-0.03134	-0.07623	-0.05848	-0.27811	0.065696	0.006873
bio16	0.237186	0.085977	0.101286	0.002275	-0.10689	-0.15391	-0.20313	-0.25666	0.089178	-0.04474	-0.01026	0.086245	0.053072
bio17	0.13619	0.229983	-0.17832	-0.2048	-0.25654	0.272902	0.019011	0.047073	-0.05109	0.121453	-0.08513	-0.03733	0.074354
bio18	0.147508	0.118817	-0.11704	0.012744	-0.48316	-0.26417	0.009688	0.322616	0.016445	-0.07861	0.019626	0.217982	0.019709
bio19	0.168017	0.145826	0.035756	-0.10786	0.107783	0.24477	-0.20906	-0.54508	0.036037	0.165442	-0.08629	-0.07788	0.03994
cec30	-0.16728	0.164914	-0.18987	0.092927	0.226154	0.121258	-0.07055	0.117738	-0.1219	0.021977	0.045034	-0.39521	0.085478
cfvo30	-0.16704	0.085882	0.29759	0.032606	0.098345	0.338476	-0.09035	-0.03517	-0.11786	0.150835	-0.26593	0.20351	-0.04154
clay30	0.153512	0.067082	-0.04364	0.348652	0.001734	0.011951	0.53855	-0.10094	0.243206	-0.0093	-0.5107	-0.08991	0.000443
elevation	-0.16104	0.076752	0.311522	0.199957	-0.34066	0.149301	-0.0177	0.006909	-0.07034	-0.02512	-0.00489	-0.19495	0.117834
nitrogen30	-0.05227	0.312026	0.00848	-0.00568	0.188308	-0.17885	-0.17758	0.183941	-0.04074	-0.00821	-0.18432	0.051514	0.1624
ocd30	-0.05273	0.320489	-0.01958	0.061128	0.201882	-0.27222	-0.05046	-0.03157	0.05554	0.100188	0.027912	-0.20307	0.129225
ocs30	0.001043	0.324382	-0.07666	0.125936	0.107179	-0.24399	-0.04898	0.015598	0.088538	0.061822	0.122289	-0.3079	0.230239
phh2o30	-0.23567	-0.10369	-0.07215	-0.01637	0.051909	0.154551	-0.08737	0.054959	-0.11982	0.118503	-0.12571	-0.00212	-0.14603
sand30	-0.11923	-0.10505	0.223434	-0.54191	0.013568	-0.09989	-0.14042	0.114683	0.090487	0.05009	0.0946	-0.0825	0.0992
silt30	0.037226	0.093855	-0.28839	0.482277	-0.02161	0.13599	-0.2789	-0.07713	-0.35209	-0.06545	0.3212	0.2019	-0.1461
slope1	-0.07464	0.191355	0.258262	0.177329	-0.02772	-0.02934	0.08239	0.164578	0.152849	0.755026	0.2052	0.2646	-0.0255
soc30	-0.00608	0.286172	-0.04986	-0.13837	0.056734	-0.10422	-0.24807	0.24136	-0.23096	-0.0565	-0.4972	0.0361	-0.3351
wrb	-0.11458	-0.0231	-0.14908	0.158556	-0.01031	0.283793	-0.41646	0.212173	0.778496	-0.13829	-0.0311	0.0080	-0.0834

DOI: 10.4206/Bosque.e4709

Table S4. Performance metrics of ecological niche modeling algorithms for *Handroanthus impetiginosus* and *Handroanthus serratifolius*.

Category	Metric/Algorithm	Original Reference
Validation metrics	AUC (Area Under the Curve)	Fielding & Bell (1997)
Validation metrics	Kappa	Cohen (1968)
Validation metrics	TSS (True Skill Statistic)	Allouche et al. (2006)
Validation metrics	Jaccard index	Leroy et al. (2018)
Validation metrics	Sorensen index	Leroy et al. (2018)
Tested algorithms	Bioclim	Nix (1986)
Tested algorithms	GLM – Generalized Linear Models	McCullagh & Nelder (1989)
Tested algorithms	MaxEnt – Maximum Entropy	Anderson & Gonzalez (2011)
Tested algorithms	Random Forest	Prasad et al. (2006)
Tested algorithms	SVM – Support Vector Machine	Prasad et al. (2006)
Tested algorithms	Bayesian Gaussian Process	Williams & Barber (1998)